DRUG ANALYTICAL RESEARCH
ISSN: 2527-2616 *www.seer.ufrgs.br/dar*

Development and Characterization of Clioquinol Nanocrystals

Francielli Lima dos Santos[a], Julia Capp Zilles[a], Simone Jacobus Berlitz[b], Irene Clemes Kulkamp Guerreiro[a,b], Alexandre Meneghello Fuentefria[a], Renata Vidor Contri[a*]

[a]*Programa de Pós-Graduação em Ciências Farmacêuticas (PPGCF), UFRGS, Porto Alegre, Brazil;*
[b]*Programa de Pós-Graduação em Nanotecnologia Farmacêutica (PPGNANO), UFRGS, Porto Alegre, Brazil*
**Corresponding author: renata.contri@ufrgs.br*

Drug nanocrystals, composed solely of active substance and stabilizer, have recently been proposed for cutaneous applications, including the management of skin fungal infections, which are often difficult to treat. Clioquinol nanocrystals suspensions were obtained using two preparation methods (small-scale wet bead milling or probe sonication), varying drug concentrations (1 or 0.1%), surfactants (poloxamer 407 or polysorbate 80), and bead sizes (0.8 and 0.3 mm). Both techniques were able of decreasing particle size, however the wet bead milling was selected as the most promising method. The drug concentration and the type of surfactant also considerably impacted the process. The selected nanocrystal suspension (bead milling, 1% drug, 1% polysorbate 80, 0.3 mm beads) exhibited an average particle size of approximately 300 nm (polydispersity index of 0.254), a zeta potential of −7.6 mV, a pH value of 5.4, a drug content of about 97% (relative to 10 mg/mL), and a nanocrystallization efficiency of approximately 96%. The nanocrystal suspension showed stability for 90 days at room temperature. Overall, the results indicate that clioquinol nanocrystals are possible to be obtained by small-scale wet bead milling and present suitable nanometric features, being considered a promising alternative as cutaneous antifungal therapy.

Keywords: Antifungal; Clioquinol; Nanosuspension; Polysorbate 80; Skin; Wet bead milling

Article received at 12/22/2025 and accepted at 04/06/2026.
https://doi.org/10.22456/dar.v10i1.152513

Introduction

The incidence of fungal infections is increasing all over the world (1), and it is estimated that approximately one billion people are affected by this kind of infection (2,3). In most cases, fungal infections are not considered a severe health issue; however, immunocompromised patients may have a higher chance of complications (2,3).

Dermatophytic fungi, non-dermatophytic fungi, and yeasts can cause dermatomycosis. Dermatophytes, which are responsible for 20-25% of reported fungal infections worldwide (4), are divided into three genera: *Epidermophyton, Trichophyton and Microsporum* (5,6). These fungi target keratinized structures such as hair, nails, and skin (4). The pathophysiology of these infections involves initial adherence to the stratum corneum (SC) facilitated by the fibrils on the cell walls of the fungal spores, subsequently leading to invasion into underlying layers (7). Besides dermatophytes, fungi of the genus Fusarium spp. (*F. solani, F. oxysporum and F. moniliforme*) can cause recalcitrant skin infections (8). Recalcitrant infections, which are hard to treat infections, involve relapses, recurrence, reinfection, persistent infection, or chronic infection, potentially leading to microbiological resistance (9).

Antifungal drugs are substances that act against infections caused by fungi. Superficial infections are commonly treated with topical antifungal agents, and the choice of the drug is determined by the site and extent of the infection (10). Topical treatment avoids adverse effects and drug interactions that can happen when drugs are orally administered. The efficacy of topical treatment using antifungal drugs is dependent on skin penetration, which is limited by the skin barrier. The skin presents low permeability to drugs due to the cohesion of the epidermal cells and the lipids of the SC (11). In this way, topical treatments often have low efficacy and require long treatment periods, which shows the need to search for new molecules and advanced formulations (12).

Several strategies are being studied to improve the drug efficacy of topical antifungal treatments, including the use of nanotechnology by means of nanoemulsions (13), polymeric nanoparticles (5,14), inorganic nanoparticles (15), liposomes (16), lipid nanoparticles (17) and nanocrystals (18–21). Drug nanocrystals are nano-sized delivery systems which consist of drug and stabilizers only (22). Nanocrystals can increase the bioavailability of drugs through oral use. Recently, this type of nanoparticles has also been proposed for cutaneous application, aiming to enhance cutaneous penetration of water-insoluble drugs (18,21–24). Miconazole nitrate nanocrystals have been developed and have proven to be more effective and capable of increasing skin penetration compared to non-nanostructured miconazole nitrate formulations (21). Permana and co-workers (2020) developed itraconazole nanocrystals and combined them with dissolving microneedles for the treatment of candidiasis, evaluating the ex vivo permeation in porcine skin (18). The combination of itraconazole nanocrystals and dissolving microneedles improved drug penetration in ex vivo infection models (18).

Clioquinol (5-chloro-7-iodo-8-quinolinol) is a substance with a broad spectrum and efficacy in the treatment of

skin mycoses (25). Clioquinol can inhibit hyphal growth, and its mechanisms of action may be associated with damage to the fungal cell wall, leading to altered membrane permeability (26). It is commercially available in cream form, usually at 1 or 3%, alone or combined with other substances (27). Despite its therapeutic potential, conventional clioquinol formulations present important limitations that may compromise their clinical efficacy. These limitations are mainly associated with its high lipophilicity and extremely low aqueous solubility (less than 0.01 mg/mL), which can restrict drug dissolution and reduce its availability at the site of action (28). In addition, topical formulations may present limited drug penetration through the stratum corneum, the main barrier of the skin. In this context, the development of nanometric drug delivery systems is an interesting strategy to overcome these limitations. Our research group developed, previously, a lipid-based clioquinol nanocarrier for the treatment of dermatomycosis, with enhanced antifungal activity against nine fungal strains tested (five yeasts and four dermatophytes) (29). It was observed that the increase in antifungal activity may result from the enhanced solubility of clioquinol within the nanometric system (29). The number of articles available in the literature on clioquinol nanoparticles are limited, highlighting the innovation of such an approach.

Therefore, the aim of the present study was to develop and characterize clioquinol nanocrystals, and to evaluate the effect of the nanocrystallization technique and parameters on the nanocrystals´ properties.

Experimental section

Materials

Polysorbate 80 and methanol were obtained from Dinâmica Química Contemporânea LTDA (Idaiatuba, Brazil). Poloxamer 407 and clioquinol were purchased from CHEMPECS Comércio e Representações (São Paulo, Brazil) and Sigma Aldrich Brasil (Cajamar, Brazil) respectively. Yttria-stabilized zirconium oxide beads 0.8 and 0.3 mm were purchased from CWL Esferas and Só Esferas, respectively (São Paulo, Brazil).

Determination of the most suitable size reduction method and drug concentration

The nanocrystals were initially obtained using two top-down techniques: small-scale wet bead milling (NCM) and probe sonication (NCS; QR350W, Eco-Sonics, Indaiatuba, SP, Brazil) (30,31) (Figure 1). These two techniques, which are described in the literature to produce nanocrystals, were selected due to their low cost, ease of execution and scaling up, and no need for organic solvent (32). For both techniques, the drug concentration (clioquinol) varied from 0.1 to 1.0%, as shown in table 1, while maintaining the surfactant (poloxamer 407) concentration at 1%. Before undergoing size reduction techniques, a drug dispersion in an aqueous surfactant solution (Crystals = CR) was obtained by simple dispersion of clioquinol into an aqueous surfactant solution, which was stirred (magnetic stirring) for 10 minutes.

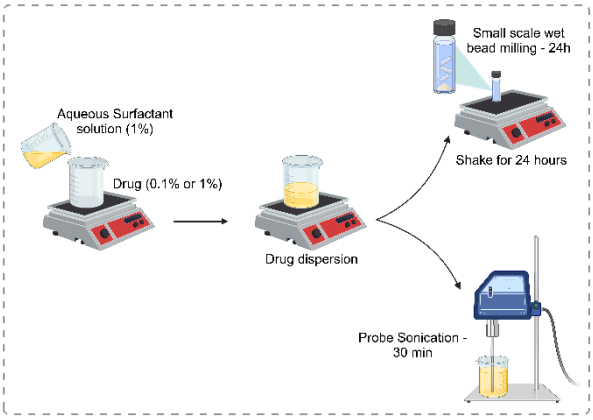

Figure 1. Techniques used for obtaining clioquinol nanocrystals (small-scale wet bead milling and probe sonication).

Table 1. Developed clioquinol nanocrystals formulations. CR=crystals; NCM= nanocrystals obtained by milling, NCS = nanocrystals obtained by sonication, NA= not applicable

Formulation	% Clioquinol	Particle size reduction technique
CR0.1	0.1	NA
CR1	1	NA
NCM0.1	0.1	Wet bead milling
NCM1	1	Wet bead milling
NCS0.1	0.1	Probe Sonication
NCS1	1	Probe Sonication

To obtain the nanocrystals by wet bead milling (NCM), a small-scale milling process was used, as reported by Romero and co-workers (2016) with modifications (31). 1.3 g of 0.8 mm or 0.3 mm yttria-stabilized zirconium oxide beads were weighed and placed into an amber glass vial (5 mL capacity). Into the vial, 3.0 mL of the drug dispersion were added along with three magnetic stirring bars. It was then stirred on a magnetic stirrer plate (FISATOM 752A) for 24 hours, at room temperature. To obtain nanocrystals using a probe sonication (NCS), the drug dispersion was brought into contact with the equipment's probe tip and immersed in an ice bath to prevent overheating of the formulation. The dispersion was sonicated for 30 minutes, with intervals of 5 minutes between each cycle of 5 minutes. The most promising technique and the percentage of drug to obtain the nanocrystals were determined based on macroscopic aspect, crystal presence under optical microscopy, and nanoparticle size measured by dynamic light scattering.

Impact of surfactant variation and bead milling size in the wet bead milling technique

To reduce the particle size, the impact of the type of surfactant was evaluated. Therefore, poloxamer 407 (the first surfactant tested) was replaced for polysorbate 80. In the same way, 0.8 mm beads were changed for 0.3 mm beads. The optimal parameters were determined based on particle size and polydispersity index (dynamic light scattering). It is well known that these two factors (surfactant type and bead size) can directly influence particle size of nanocrystals (32).

Characterization of the developed clioquinol nanocrystals

The most suitable nanocrystal suspension (NC-CL) was characterized, in triplicate of batches, regarding its average particle diameter and particle size distribution by dynamic light scattering using Zetasizer® Nano ZS equipment (Malvern Instruments, Worcestershire, UK). This technique allows the determination of the hydrodynamic radius of a hypothetical solid particle by scattering light with the same intensity as the particles under investigation while diffusing in the dispersion (33). The samples were diluted (1:100; v/v) in a saturated solution of clioquinol (previously obtained and filtered with 0.45 µm filter), to ensure no dissolution of the nanocrystals during the analysis (34). The same equipment was used to measure the zeta potential by electrophoretic mobility. The samples were diluted (1:100; v/v) in a 10 mM NaCl solution, previously filtered with a 0.45 µm filter, according to ASTM guidelines (35). The determination of particle diameter, particle size distribution and zeta potential were performed at 25°C. The pH measurements were conducted directly using MQuant® pH measurement strips (Acilit Ph 0-6, MERCK), considering the sample limitation of each batch (2.5mL). The suspensions were analyzed using an optical microscope (Olympus CX31) to determine the presence or absence of micrometer-sized particles. To evaluate the morphology of nanocrystals, scanning electron microscopy (SEM) was applied (Zeiss EVO MA-10, Zeiss) (18). For the analysis, stubs were used, and a carbon tape was applied in each of them, followed by adding a drop of the formulations (undiluted or diluted with purified water (1:100)) to be analyzed. After 48 hours of drying at 25°C, the samples were gold-coated and analyzed.

Clioquinol quantification and method validation

To determine the drug content and nanocrystallization efficiency, a UV-Vis spectrophotometer (UV-2600 UV-VIS spectrophotometer, Shimadzu, Japan) was used (29). The measurements were performed in quartz cuvettes with a chamber volume of 3.5 mL, uncovered, at a wavelength of 254 nm (29). The analytical method was validated according to guidelines Q2 (R1) of the International Conference on Harmonization (ICH) (36). A drug stock solution (1 mg/mL) was prepared in methanol. Linearity, specificity, precision (intraday and interday), and accuracy were evaluated. Regarding linearity, three calibration curves (ranging from 2 to 8 µg/mL) were obtained. The specificity was evaluated by analyzing a surfactant solution at the wavelength used (254 nm), as the nanocrystals consist solely of clioquinol and polysorbate 80. For intraday precision, six solutions of 4 µg/mL were evaluated on the same day with the same experimental conditions, and, for interday precision, three solutions of 4 µg/mL were prepared on three different days, with a total of nine samples. The precision results were evaluated in terms of relative standard deviation (RSD). The accuracy was determined by adding 50 µL of polysorbate 80 solution (1 mg/mL) to the diluted clioquinol stock solution (2, 4, and 8 µg/mL). Analyses were performed in triplicate on the same day. The accuracy results were evaluated in terms of the percentage recovered and its RSD.

Drug content was evaluated by diluting a sample of the nanocrystals in methanol, followed by 10 minutes in an ultrasound bath at 25°C, and analyzed for drug quantification by UV-Vis spectrophotometry. The drug's nanocrystallization efficiency was determined after centrifuging 100 µL of the nanocrystals for 10 minutes (Smart Personal Centrifuge, Gandhinaga, India) at 25°C. An aliquot of the supernatant, which contained only the solubilized form of the drug, was diluted 1:100 using methanol and then analyzed for drug quantification by UV-Vis spectrophotometry. Nanocrystallization efficiency was obtained by subtracting the soluble drug concentration from the total drug concentration (the drug content) as described in Equation (1).

$$Nanocrystallization\ efficiency\ (\%) = \frac{Total\ Drug\ Concentration - Soluble\ Concentration}{Total\ Drug\ Concentration} * 100 \quad (1)$$

Stability of clioquinol nanocrystals

For the stability study, the formulations were stored at room temperature (25°C, BOD incubator, Cienlab®, Brazil) on amber glass flasks and reanalyzed after 30 and 90 days of storage, regarding particle size and polydispersity index, zeta potential, drug content, and nanocrystallization efficiency.

Statistical Analysis

Statistical analysis was performed using one-way and two-way analysis of variance (ANOVA) followed by Tukey's test using GraphPad Prism® 8.01 (San Diego, CA, USA).

Results and Discussion

Development of clioquinol nanocrystals formulation

The developed suspensions, as well as the drug concentrations, and the techniques used for obtaining nanocrystals, are described in Table 1. Similarly, the techniques for obtaining the nanocrystals is illustrated in Figure 1. The nanocrystals suspensions exhibited an opaque appearance, with a lower percentage of the drug leading to a more translucent formulation (NCM0.1 and

NCS0.1). The formulations obtained through wet bead milling (NCM0.1 and NCM1) exhibited a greenish/yellowish color, while the formulations obtained with probe sonication (NCS0.1 and NCS1) appeared white/slightly yellow. The difference in color among formulations may be attributed to particle size differences, a phenomenon observed in certain materials (38). Upon standing for 10 minutes, precipitation occurred in all samples.

The two different techniques that were selected to develop the clioquinol nanocrystals were chosen due to their low cost, ease of execution, and no need of organic solvents, as well as being well-described in the literature for the production of nanocrystals (32). The ultrasound technique (probe sonication) is an efficient method to break drug particles into smaller particles through the vibration of acoustic waves (39). This technique is easily operated in the laboratory and highly reproducible (32). Various factors affect the size of nanocrystals, including the cavitation depth, horn immersion depth, horn length, and ultrasound treatment (32,39). Limitations of the ultrasound technique include difficulty in scalability, and the fact that very high ultrasound energy increases collisions, agglomerations, and sizes of particles (32,40).

On the other hand, the wet milling process uses mechanical attrition to wet particles by using an aqueous solution of surfactants or stabilizers and shearing as well as ground via using milling balls in a milling container (32). Furthermore, the technique could be scalable. Antifungal nanocrystals are well described in the literature by wet milling process (18,21,41). The limitations of the wet milling process include a decrease in drug crystallinity, a long period of operation, a high energy input, and the possible contamination from erosion of milling pearls or balls (32,42).

Concerning the determination of the particle sizes by dynamic light scattering, it was not possible to obtain measurements for the samples before the nanocrystallization (CR) and for the ones obtained through probe sonication (NCS), indicating a considerable micrometric population within these samples. The formulations obtained through wet bead milling presented an average particle size of around 600 nm (NCM0.1 = 601 nm, NCM1 = 557 nm), with high polydispersity index (PDI) values (0.33 for NCM0.1 and 0.42 for NCM1). Therefore, the wet bead milling technique was considered more promising in the development of clioquinol nanocrystals. However, further improvement was considered necessary.

In the study described by Romero and co-workers (2016), it was observed that the final particle size obtained by the same technique (small scale bead milling) varies depending on the drug used and the milling period (31). The smallest particle size obtained varied from 49 nm to 294 nm for the different drugs and milling periods (31). Additionally, the milling time varied for each drug, and it was also observed that after a certain period of milling, the nanocrystals began to aggregate, increasing their size (31).

Considering the probable presence of a micrometer-sized population, indicated by the high PDI values, the nanocrystals were examined using an optical microscope to verify the presence or absence of micrometer-sized particles, as can be seen in Figure 2. From the images obtained, it was possible to notice that both techniques were effective in reducing the size of the drug crystals. However, an undesirable micrometer-sized population persists in all samples. Through the comparison of images, it was confirmed that the wet bead milling technique was more effective in reducing particle size than the probe sonication, regardless of drug concentration, which was already observed with dynamic light scattering analysis. Therefore, considering the high drug concentration, NCM1 appeared to be the most promising for the continuation of the studies.

In view of the need to improve the formulation, the impact of surfactant exchange was also evaluated. It was possible to reduce the size of the nanocrystals as well as the PDI by switching from poloxamer 407 to polysorbate 80. The particle size of the nanocrystals decreased from 557 nm (PDI 0.42) to 276 nm (PDI 0.283), using 0.8 mm yttria-stabilized zirconium oxide beads. The choice of the surfactant is an important step in the nanocrystal's development as the surfactant plays a crucial role in the particle size. Drug nanocrystals are formed from a solid core surrounded by a stabilizer layer, and typical stabilizers are amphiphilic surfactants or polymers (43). The nanocrystals formation creates high energy surfaces, which can turn to aggregation and Ostwald ripening if stabilization is not efficient. Surfactants are a crucial component in nanocrystals production, and they are amphiphilic molecules characterized by a hydrophilic head group (ionic or non-ionic) and a hydrophobic tail (44). The success of the stabilizer is highly dependent on the drug, meaning that the drug and the stabilizer must exhibit a certain degree of affinity (43).

Poloxamers are synthetic polymers composed of two polyoxyethylene (PEO) parts and one polyoxypropylene (PPO) moiety arranged in a basic PEO-PPO-PEO architecture (45), and they have been explored and applied in the nanocrystals production (21,46,47). Poloxamer 407 has been shown to effectively stabilize nanoparticles. However, its stabilizing efficiency can vary depending on the specific formulation and conditions (44). On the other hand, polysorbates are nonionic surfactants with 1-3 fatty acids attached to polyethoxylated sorbitan (45). Polysorbate 80 is highly effective in the production of nanocrystals due to its amphiphilic structure, which allows it to adsorb onto nanoparticles surfaces, reducing interfacial tension and preventing aggregation. Poloxamer 407 and polysorbate 80 could be effective stabilizers for nanocrystals, influencing particle size and stabilization; however, other formulation parameters

can also affect the nanocrystals properties, such as the active substance used.

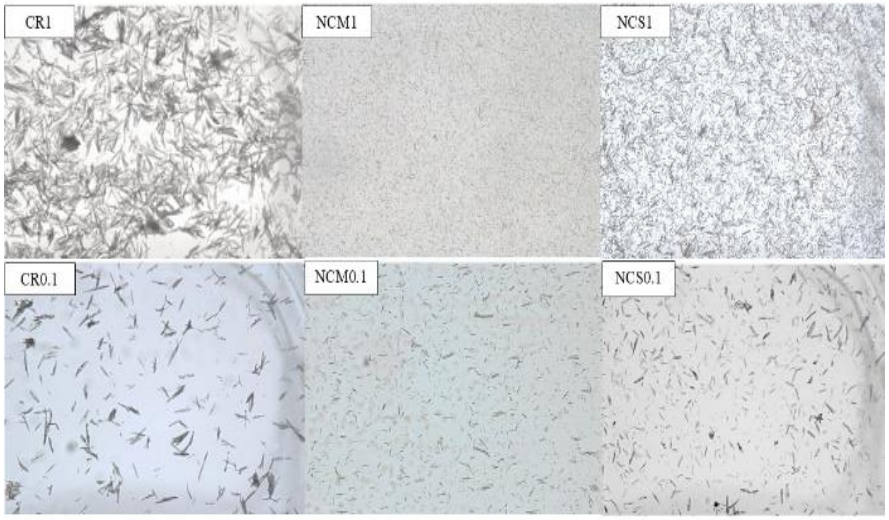

Figure 2. Optical microscopy images (magnification of 40X) of suspensions obtained with probe sonication (NCS) and wet bead milling (NCM), with 1% (1) and 0.1% (0.1) clioquinol. Clioquinol crystals before nanocrystallization (CR) are also shown. All formulations were obtained with poloxamer 407 and, for wet bead milling, 0.8 mm Yttria-stabilized zirconium oxide beads were applied.

The impact of the surfactant on the particle size was studied by other authors (20,21,48). Anjani and co-workers (2022) evaluated the influence of five surfactants (Lutrol® F108, pluronic®F88 Pastille, poly (vinyl alcohol)-PVA, Soluplus®, and Tween®80) in the particle size of metronidazole nanocrystals (20). The surfactants Tween®80, Lutrol®F108, and Pluronic®F88 Pastille resulted in very similar drug particle sizes (20). The surfactant Soluplus® resulted in a drug particle smaller than 100 nm (20). The authors attributed the reduction in the drug particle size to the combination of physical attrition due to media-milling along with the enhancement in the drug solubilizing effect of Soluplus® (20). Pyo and co-workers (2017) also evaluated the influence of six surfactants (poloxamer 188, poloxamer 407, Planctare®810UP, Planctare®2000UP, Tween®80, and Miranol®Ultra C32) in the particle size of miconazole nitrate nanocrystals (21). The surfactants poloxamer 407 and Tween® 80 were able to produce miconazole nitrate nanocrystals with suitable particle size (around 300 nm) and PDI (around 0,3) (21).

The influence of reducing the size of milling beads (from 0.8 mm to 0.3 mm, considering the use of polysorbate 80 surfactant) was also analyzed, resulting in nanocrystals with a size of 305 nm and PDI of 0.251. The size of the beads is an important factor in reducing the crystals to the nanometric scale. Romero and co-workers (2016) affirm that the particle size of nanocrystals decreases with the use of smaller-sized beads (31). Narayan and co-workers (2017) also evaluated the impact of the milling time and the use of smaller beads, and the authors concluded that particle size was decreased with longer milling time (from 1 to 4h) and smaller milling beads (from 15 to 5 mm) (49). The size reduction in wet milling depends on the number and intensity of collisions between the drug particles, and the milling beads the higher collision frequencies are due to their increased surface area-to-volume ratio (42). As smaller beads move faster, their ability to break down crystals into smaller particles becomes more efficient (31). In the present study, no reduction in the average particle size was observed when using smaller beads; however, a lower PDI was achieved. The lower the PDI, the more uniform the particle size distribution, while higher values suggest a broader range of sizes (33).

Therefore, the 1% clioquinol nanocrystals formulation obtained by wet bead milling using 0.3 mm beads and polysorbate 80 (1%) as a surfactant was determined to be the most suitable formulation, and such suspension was obtained in triplicate of batches for further characterization.

Clioquinol quantification/determination method validation

The UV-VIS spectrophotometric method was considered specific for quantifying clioquinol in the nanocrystal suspension, as the polysorbate 80 solution did not show absorbance at the wavelength of 254 nm. The method demonstrated linearity with an R-value of 0.9996 and showed repeatability and intermediate

precision with RDS values of 2.87% and 2.93%, respectively. The accuracy was considered adequate for the methodology with an RSD of 2.39%. These values are in accordance with those stipulated by ICH (36).

Characterization and stability of the developed clioquinol nanocrystals

The results for particle size, size distribution, zeta potential, pH, drug content, and nanocrystallization efficiency evaluated right after obtainment and for 90 days under storage are shown in Table 2.

Table 2. Characterization of the selected clioquinol nanocrystals suspension (NC-CL).

Evaluated Parameters	Day 0	Day 30	Day 90
Z average (nm)	307 ± 2.5	327 ± 17.8	331 ± 10.9
PDI	0.254 ± 0.02	0.266 ± 0.02	0.256 ± 0.02
Zeta potential (mv)	-7.6 ± 2.0	-5.6 ± 0.9	-6.8 ± 6.8
pH	5.4 ± 0.3	5.2 ± 0.2	5.8 ± 0.3
Drug content (%)	97.3 ± 6.4	95.6 ± 9.3	100.1 ± 7.9
Nanocrystallization Efficiency (%)	96.1 ± 1.2	96.83 ± 0.7	97.5 ± 1.9

The macroscopic aspect of CR-CL (before the wet milling process, clioquinol crystals) and NC-CL (clioquinol nanocrystals) are shown in Figure 3.

As described before, the NC-CL exhibited a greenish/yellowish color, whereas before milling (CR-CL), the suspension exhibited a more whitish coloration. The particle size of the nanocrystals was around 300 nm, with an adequate monomodal size distribution (PDI around 0.25) as demonstrated in Figure 4. In contrast, the particle size of a lipid-based nanocarrier containing clioquinol developed by Berlitz and co-workers (2023) was approximately 91 nm, with a particle size distribution of 0.102 (29). Nevertheless, it is important to note that this is a different type of nanometric system. The literature reports variable particle sizes and size distributions for antifungal nanocrystals (18,19,21,41). Pyo and co-workers (2017) and Permana and co-workers (2020) developed miconazole nitrate and itraconazole nanocrystals, respectively, using a similar wet bead milling technique, obtaining nanocrystals with analogous particle sizes (346 and 352 nm) but higher size distributions (0.39 and 0.37) compared to the present study (18,21). Patel and co-workers (2019) developed clotrimazole nanocrystals using media milling technique for the treatment of cutaneous candidiasis achieving a similar particle size (264 nm) and size distribution (0.211) (41).

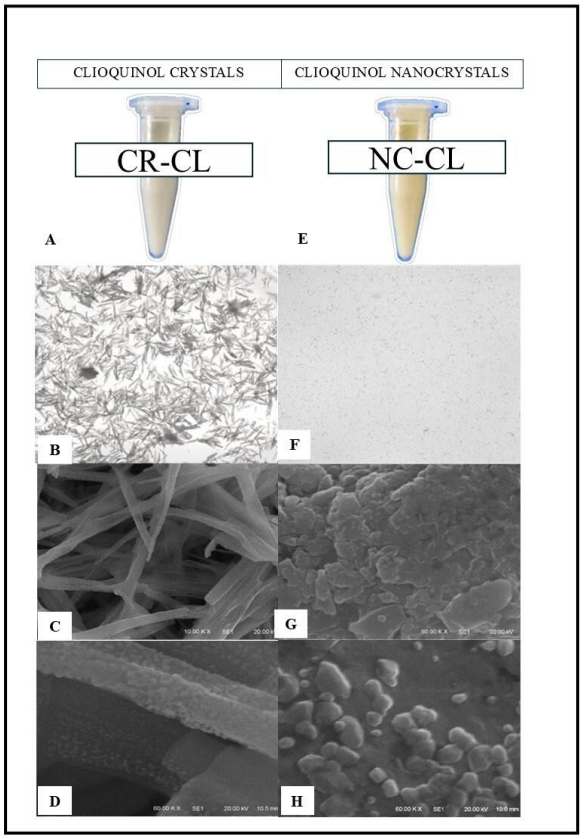

Figure 3. Macroscopic aspect, optical microscopy and Scanning Electron Microscopy before (Crystals) and after (Nanocrystals) wet bead milling. A: Macroscopic aspect of Clioquinol Crystals (CR-CL); B: Optical Microscopy of Clioquinol Crystals 40X (CR-CL); C: Scanning Electron Microscopy of CR-CL 10,000x; D: Scanning Electron Microscopy of CR-CL 60,000x; E: Macroscopic aspect of Clioquinol Nanocrystals (NC-CL); F: Optical Microscopy of Clioquinol Nanocrystals 40X (NC-CL); G: Scanning Electron Microscopy of NC-CL 60,000x; H: : Scanning Electron Microscopy of NC-CL (diluted 1:100 in purified water) 60,000x.

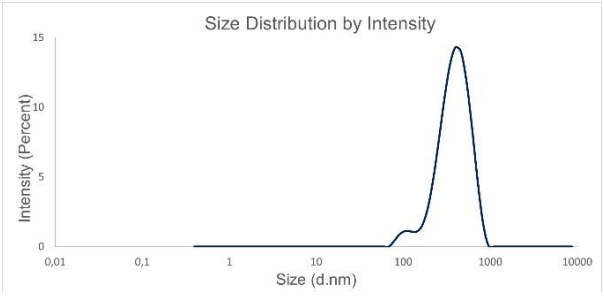

Figure 4. Particle size distribution of clioquinol nanocrystals (NC-CL) obtained by dynamic light scattering.

The zeta potential was around -7 mV. The nanocrystals were developed using polysorbate 80, a non-ionic surfactant, which likely resulted in low zeta potential values due to the presence of a constant hydrophobic group in its composition (50,51). In systems stabilized with non-ionic surfactants, low zeta potential values are

expected, and colloidal stability is primarily governed by steric rather than electrostatic mechanisms (41). Berlitz and co-workers (2023) also used a non-ionic surfactant (poloxamer 407) to produce the lipid-based nanocarrier and obtained a low zeta potential (around -9 mV) (29). Campos and co-workers developed a clioquinol-loaded P(MMA-co-AA) nanoparticle with a zeta potential value of -58 mV (52). The negative value of the zeta potential is due to the use of an anionic surfactant (sodium dodecyl sulfate (SDS)), and values greater than 50 mV, in module function, indicates that the particle stabilization is primarily due to charge repulsion (52). The authors affirm that the surface charge of the nanoparticles was predominantly attributed to the surfactant (sodium dodecyl sulfate) (52).

The pH value of NC-CL was around 5, an adequate value for skin application since pH values between 4.1 and 5.8 are considered ideal for topical application (53). The drug content was 97.3% of the theoretical content (10 mg/mL), and the nanocrystallization efficiency was high (96%), indicating that almost 100% of the drug is nanocrystallized. Therefore, around 4% of the drug content (0.38 mg/mL) is solubilized in the aqueous medium, probably due to the presence of polysorbate 80, considering the clioquinol aqueous solubility is less than 0.01 mg/mL according to Padmanabhan, Becue and Smith (1990) (28).

The stability was evaluated during 90 days at room temperature (25°C), and there was no statistical difference in any of the evaluated data, demonstrating that NC-CL is stable for at least 90 days at the temperature condition analyzed. Although the zeta potential values were relatively low, which is expected due to the use of a non-ionic surfactant, the high stability of the clioquinol nanocrystals suggests that steric stabilization plays a predominant role in maintaining formulation stability. The presence of polysorbate 80 likely promotes the formation of an adsorbed layer around the nanocrystals, preventing aggregation and crystal growth over time (50).

Pyo and co-workers (2017) evaluated the stability of miconazole nitrate nanocrystals during 90 days at 4°C, 25 °C and 40°C (21). The authors determined that nanocrystals stored in the fridge (4°C) were more stable than those stored at 25°C or 40°C, preventing crystal aggregation and consequently maintaining particle size (21). The process of nanonization creates particles with higher surface area, which, if not properly stabilized using an appropriate surfactant, tend to aggregate owing to Ostwald ripening (41). An ideal surfactant should have adequate affinity towards the surface of the drug particles to stabilize the drug (41). Polysorbate 80 enhances the wettability of the particles and forms a thin adsorption layer around the hydrophobic drug, aiding in the dispersion of aggregates formed during milling through steric stabilization (41). Therefore, polysorbate 80 was considered an appropriate surfactant, as there was no increase in particle size over 90 days at room temperature. Thus, refrigeration was not considered necessary for NC-CL. The stability results obtained in our study stand out compared to those described in the literature, as no statistically significant changes were observed in the parameters analyzed after a 90-day storage period at room temperature.

Microscopic techniques are among the most popular characterization approaches, facilitating the evaluation of surface morphology and microstructure of various micro or nano vehicles (54). Optical and scanning electron microscopy were employed to assess particle size reduction and morphology of NC-CL. Comparisons of the images obtained from optical microscopy indicate that the chosen technique was effective in reducing the size of the drug crystals into nanocrystals, as shown in Figure 3 (B and F), with no micrometer-sized particles observed in the nanosuspension. Pyo and co-workers (2019) also used optical microscopy to evaluate the presence of crystals or nanocrystal agglomeration in developed nanocrystal formulations (21).

The morphology of NC-CL was evaluated and identified using scanning electron microscopy (SEM) as shown in Figure 3. The SEM analysis reveals a great reduction in the particle size of the crystals when comparing CR-CL (C and D) with NC-CL (G and H). The nanocrystals were evaluated with (Figure 3H) and without dilution in purified water (Figure 3G). In Figure 3G, the nanocrystals appear clustered together, while in Figure 3H, after dilution, they are dispersed into individual units. SEM imagens reveal that CR-CL exhibited a morphology like that observed under optical microscopy (thin and elongated, as shown in Figure 3C and 3D). However, upon size reduction, the nanocrystals displayed a more rounded morphology (Figure 3G and H). Yao and co-workers and Permana and co-workers (2021) also evaluated the morphology of azoxystrobin and itraconazole, respectively, using SEM (18,55).

Conclusions

This study successfully developed clioquinol nanocrystals (10 mg/mL) using small-scale wet bead milling. The nanocrystals showed suitable physicochemical stability for up to 90 days at room temperature, with high drug content and efficient nanocrystallization. The findings indicate that the developed nanosystem is a promising strategy for improving the delivery of clioquinol. However, further studies, including antifungal activity assays are necessary to confirm its therapeutic potential for the topical treatment of skin fungal infections.

Author contributions

F.L.S.: Conceptualization, Methodology, Investigation, Data curation, Formal analysis, Visualization, Writing – original draft. **J.C.Z.:** Investigation, Data curation, Writing – review and editing. **S.J.B.:** Investigation, Validation, Writing – review and editing. **I.C.K.G.**:

Methodology, Resources, Writing – review and editing. **A.M.F**.: Conceptualization, Resources, Supervision, Writing – review and editing. **R.V.C.:** Conceptualization, Supervision, Project administration, Funding acquisition, Writing – review and editing.

Conflict of Interest

The authors declare no conflict of interest.

Funding

This research was funded by Conselho Nacional de Desenvolvimento Científico e Tecnológico (423066/2018–8) and Fundação de Amparo à Pesquisa do Estado do Rio Grande do Sul (23/2551-0000953-6). This study was financed in part by the Coordenação de Aperfeiçoamento de Pessoal de Nível Superior–Brazil (CAPES) Finance Code 001 (FLS scholarship).

References

1. Lockhart SR, Guarner J. Emerging and reemerging fungal infections. Semin Diagn Pathol 2019; 36:177–81.
2. Chang YL, Yu SJ, Heitman J, Wellington M, Chen YL. New facets of antifungal therapy. Virulence 2017; 8:222–36.
3. Rabaan AA, Sulaiman T, Al-Ahmed SH, Buhaliqah ZA, Buhaliqah AA, AlYuosof B, et al. Potential Strategies to Control the Risk of Antifungal Resistance in Humans: A Comprehensive Review. Antibiotics (Basel) 2023;12.
4. Alehashemi R, Arghavan B, Abastabar M, Niknejad F, Aghili SR. Molecular epidemiology of dermatophytosis in Golestan, Iran: A cross-sectional study. Microb Pathog 2025; 199:107223.
5. dos Santos FL, Zilles JC, Machado AU, Marques MS, da Costa BS, Kulkamp Guerreiro IC, et al. Polymeric Nanocapsules Containing Ozonated Oil and Terbinafine Hydrochloride as a Potential Treatment Against Dermatophytes. AAPS PharmSciTech 2023; 24:1–12.
6. Özcan I, Abaci Ö, Uztan AH, Aksu B, Boyacioğlu H, Güneri T, et al. Enhanced topical delivery of terbinafine hydrochloride with chitosan hydrogels. AAPS PharmSciTech 2009; 10:1024–31.
7. Jazdarehee A, Malekafzali L, Lee J, Lewis R, Mukovozov I. Transmission of Onychomycosis and Dermatophytosis between Household Members: A Scoping Review. Journal of Fungi 2022, Vol 8, Page 60 2022;8:60.
8. Dignani MC, Anaissie E. Human fusariosis. Clinical Microbiology and Infection 2004; 10:67–75.
9. Kumar S, Kaur A, Kaur S. Autoimplantation Therapy in Extensive and Recalcitrant Dermatophytosis: A Case Series. J Clin Aesthet Dermatol 2021; 14:34.
10. Meis JFGM, Verweij PE. Current management of fungal infections. Drugs 2001; 61:13–25.
11. Gupta AK, Cooper EA. Update in antifungal therapy of dermatophytosis. Mycopathologia 2008; 166:353–67.
12. Lipner SR, Scher RK. Efinaconazole in the treatment of onychomycosis. Infect Drug Resist 2015; 8:163–72.
13. Alghaith AF, Alshehri S, Alhakamy NA, Hosny KM. Development, optimization and characterization of nanoemulsion loaded with clove oil-naftifine antifungal for the management of tinea. Drug Deliv 2021; 28:343–56.
14. Tayel SA, El-Nabarawi MA, Tadros MI, Abd-Elsalam WH. Positively Charged Polymeric Nanoparticle Reservoirs of Terbinafine Hydrochloride: Preclinical Implications for Controlled Drug Delivery in the Aqueous Humor of Rabbits. AAPS PharmSciTech 2013; 14:782.
15. Agarwal A, Ramachandran S, Kumar S, Swaminathan S, Ramalingam R. A Comparative Study on Centella Asiatica-Mediated Green Synthesis of Silver and Copper Oxide Nanoparticles: Implications for Wound Healing. Particle & Particle Systems Characterization 2025:2400215.
16. Bezerra CF, Geraldo de Alencar Júnior J, de Lima Honorato R, Lucas dos Santos AT, Pereira da Silva JC, Gusmão da Silva T, et al. Antifungal effect of the liposome encapsulation of the Trans-Caryophylene and its association with fluconazole. Chem Biol Interact 2023;373.
17. Passos JS, Martino LC, Dartora VFC, Araujo GLB de, Ishida K, Lopes LB. Development, skin targeting and antifungal efficacy of topical lipid nanoparticles containing itraconazole. Eur J Pharm Sci 2020;149.
18. Permana AD, Paredes AJ, Volpe-Zanutto F, Anjani QK, Utomo E, Donnelly RF. Dissolving microneedle-mediated dermal delivery of itraconazole nanocrystals for improved treatment of cutaneous candidiasis. European Journal of Pharmaceutics and Biopharmaceutics 2020; 154:50–61.
19. Kumar M, Shanthi N, Mahato AK, Soni S, Rajnikanth PS. Preparation of luliconazole nanocrystals loaded hydrogel for improvement of dissolution and antifungal activity. Heliyon 2019;5:e01688.
20. Anjani QK, Sabri AH Bin, Domínguez-Robles J, Moreno-Castellanos N, Utomo E, Wardoyo LAH, et al. Metronidazole nanosuspension loaded dissolving microarray patches: An engineered composite pharmaceutical system for the treatment of skin and soft tissue infection. Biomaterials Advances 2022;140.
21. Pyo SM, Hespeler D, Keck CM, Müller RH. Dermal miconazole nitrate nanocrystals – formulation development, increased antifungal efficacy & skin penetration. Int J Pharm 2017; 531:350

22. Duarte PAF, dos Santos FL, Kulkamp Guerreiro IC, Fuentefria AM, Contri RV. Drug nanocrystals: A review of their application in the topical treatment of skin infections. International Journal of Nano Dimension 2025; 16:1-12.
23. Pireddu R, Caddeo C, Valenti D, Marongiu F, Scano A, Ennas G, et al. Diclofenac acid nanocrystals as an effective strategy to reduce in vivo skin inflammation by improving dermal drug bioavailability. Colloids Surf B Biointerfaces 2016; 143:64–70.
24. Vidlářová L, Romero GB, Hanuš J, Štěpánek F, Müller RH. Nanocrystals for dermal penetration enhancement – Effect of concentration and underlying mechanisms using curcumin as model. European Journal of Pharmaceutics and Biopharmaceutics 2016; 104:216–25.
25. Pippi B, Reginatto P, Da Rosa Monte MacHado G, Bergamo VZ, Dalla Lana DF, Teixeira ML, et al. Evaluation of 8-Hydroxyquinoline Derivatives as Hits for Antifungal Drug Design. Med Mycol 2017; 55:763–73.
26. Pippi B, Merkel S, Staudt KJ, Teixeira ML, de Araújo BV, Zanette RA, et al. Oral clioquinol is effective in the treatment of a fly model of Candida systemic infection. Mycoses 2019; 62:475–81.
27. You Z, Ran X, Dai Y, Ran Y. Clioquinol, an alternative antimicrobial agent against common pathogenic microbe. J Mycol Med 2018; 28:492–501.
28. Padmanabhan G, Becue I, Smith JB. Clioquinol. Analytical Profiles of Drug Substances and Excipients 1990; 18:57–90.
29. Jacobus Berlitz S, Reginatto P, Machado G da RM, Fuentefria AM, Morisso FDP, Contri RV, et al. Development of a Clioquinol Nanocarrier as a New, Promising Option for the Treatment of Dermatomycosis. Pharmaceutics 2023;15.
30. Ige PP, Baria RK, Gattani SG. Fabrication of fenofibrate nanocrystals by probe sonication method for enhancement of dissolution rate and oral bioavailability. Colloids Surf B Biointerfaces 2013; 108:366–73.
31. Romero GB, Keck CM, Müller RH. Simple low-cost miniaturization approach for pharmaceutical nanocrystals production. Int J Pharm 2016; 501:236–44.
32. Alnaim AS. Nanocrystals in Dermal Drug Delivery: A Breakthrough for Enhanced Skin Penetration and Targeted Skin Disorder Treatments. Pharmaceutics 2024; 16:1561.
33. Bhattacharjee S. DLS and zeta potential – What they are and what they are not? Journal of Controlled Release 2016; 235:337–51.
34. Zhai X, Lademann J, Keck CM, Müller RH. Nanocrystals of medium soluble actives—Novel concept for improved dermal delivery and production strategy. Int J Pharm 2014; 470:141–50.
35. ASTM International. Standard Guide for Measurement of Electrophoretic Mobility and Zeta Potential of Nanosized Biological Materials 1 2018.
36. ICH. ICH Harmonised Guideline Validation of Analytical Procedures Q2(R2). VALIDATION OF ANALYTICAL PROCEDURES, 2023
37. CLSI. M38 Filamentous Fungi Antifungal Susceptibility Test 2017:62. https://clsi.org/standards/products/microbiology/documents/m38/ (accessed April 5, 2023).
38. Khan I, Saeed K, Khan I. Nanoparticles: Properties, applications and toxicities. Arabian Journal of Chemistry 2019; 12:908–31.
39. Ran Q, Wang M, Kuang W, Ouyang J, Han D, Gao Z, et al. Advances of Combinative Nanocrystal Preparation Technology for Improving the Insoluble Drug Solubility and Bioavailability. Crystals 2022; 12:1200.
40. Thorat AA, Dalvi S V. Liquid antisolvent precipitation and stabilization of nanoparticles of poorly water-soluble drugs in aqueous suspensions: Recent developments and future perspective. Chemical Engineering Journal 2012;181–182:1–34.
41. Patel V, Sharma OP, Mehta TA. Impact of Process Parameters on Particle Size Involved in Media Milling Technique Used for Preparing Clotrimazole Nanocrystals for the Management of Cutaneous Candidiasis. AAPS PharmSciTech 2019;20.
42. Peltonen L. Design Space and QbD Approach for Production of Drug Nanocrystals by Wet Media Milling Techniques. Pharmaceutics 2018, Vol 10, Page 104 2018;10:104.
43. Tuomela A, Hirvonen J, Peltonen L. Stabilizing Agents for Drug Nanocrystals: Effect on Bioavailability. Pharmaceutics 2016;8.
44. Cortés H, Hernández-Parra H, Bernal-Chávez SA, Del Prado-Audelo ML, Caballero-Florán IH, Borbolla-Jiménez F V., et al. Non-Ionic Surfactants for Stabilization of Polymeric Nanoparticles for Biomedical Uses. Materials 2021; 14:3197.
45. Ćirin D, Krstonošić V, Poša M. Properties of poloxamer 407 and polysorbate mixed micelles: Influence of polysorbate hydrophobic chain. Journal of Industrial and Engineering Chemistry 2017; 47:194–201.
46. Omolo CA, Kalhapure RS, Agrawal N, Rambharose S, Mocktar C, Govender T. Formulation and Molecular Dynamics Simulations of a Fusidic Acid Nanosuspension for Simultaneously Enhancing Solubility and Antibacterial Activity. Mol Pharm 2018; 15:3512–26.
47. Liu X, Gan H, Hu C, Sun W, Zhu X, Meng Z, et al. silver sulfadiazine nanosuspension-loaded thermosensitive hydrogel as a topical antibacterial agent. Int J Nanomedicine 2019; 14:289.
48. Ahmed IS, Elnahas OS, Assar NH, Gad AM, Hosary R El. Nanocrystals of Fusidic Acid for Dual Enhancement of Dermal Delivery and

Antibacterial Activity: In Vitro, Ex Vivo and In Vivo Evaluation. Pharmaceutics 2020;12.
49. Narayan R, Pednekar A, Bhuyan D, Gowda C, Koteshwara KB, Nayak UY. A top-down technique to improve the solubility and bioavailability of aceclofenac: in vitro and in vivo studies. Int J Nanomedicine 2017; 12:4921–35.
50. Barradas TN, Campos VEB, Senna JP, Coutinho CSC, Tebaldi BS, Silva KGH, et al. Development and characterization of promising o/w nanoemulsions containing sweet fennel essential oil and non-ionic sufactants. Colloids Surf A Physicochem Eng Asp 2015; 480:214–21.
51. Sis H, Birinci M. Effect of nonionic and ionic surfactants on zeta potential and dispersion properties of carbon black powders. Colloids Surf A Physicochem Eng Asp 2009; 341:60–7.
52. Campos IMF, de Barros IR, Ferraz HC, Pinto JC. P(MMA-co-AA) Nanoparticles Loaded with Clioquinol and Functionalized with TAT Peptide. Macromol React Eng 2020; 14:1900046.
53. Proksch E. pH in nature, humans and skin. J Dermatol 2018; 45:1044–52.
54. Falsafi SR, Rostamabadi H, Assadpour E, Jafari SM. Morphology and microstructural analysis of bioactive-loaded micro/nanocarriers via microscopy techniques; CLSM/SEM/TEM/AFM. Adv Colloid Interface Sci 2020 ;280:102166.
55. Yao J, Cui B, Zhao X, Wang Y, Zeng Z, Sun C, et al. Preparation, characterization, and evaluation of azoxystrobin nanosuspension produced by wet media milling. Applied Nanoscience (Switzerland) 2018; 8:297–307.